X-ray Imaging Sensor using CdTe Crystals for Dual Energy X-ray Absorptiometry

Tetsuro Ohtsuchi, Hiroshi Tsutsui, Koichi Ohmori, and Sueki Baba

Abstract—**We have designed and built a multi-channel cadmium telluride detector array to test its suitability as an X-ray imaging sensor for dual energy X-ray absorptiometry. The X-ray imaging sensor was constructed of 64 CdTe detector elements with high frequency current amplifiers, discriminators, and counters. The detector elements were operated in the photon counting mode and output pulses induced by the X-ray photons were separated into two energy levels according to their height. The energy resolution of the detector elements was 18.7% to 59.54 keV gamma-rays. In combination with a K-edge filter to produce dual energy X-rays, the X-ray imaging sensor was able to generate two energy X-ray images simultaneously over a short time. By applying a simple energy subtraction method to these images, bone phantoms were distinguished from the overlying tissue phantoms and their densities could be successfully measured. It was clearly demonstrated that this X-ray imaging sensor using CdTe crystals has good potential for high speed bone densitometry.**

I. Introduction

DUAL energy X-ray absorptiometry and imaging are used mainly in the selective imaging and measuring of bone and tissue in the medical field [1], [2]. Two factors are important when carrying out dual energy X-ray absorptiometry. One is the method used to generate dual energy X-rays. Switching of the X-ray source voltage has up to now been used in both dual energy radiography [1] and in X-ray computerized tomography. The filters to attenuate low energy X-rays are used with different tube voltages to obtain pseudo-monoenergetic X-rays. K-edge filters have also been applied to the dual energy X-rays, to separate Bremsstrahlung X-rays into low and high energy regions [2], [3]. By using K-edge filters, it is possible to irradiate simultaneously with low and high energy photons.

The other factor is the use of X-ray sensors able to discriminate between X-ray energies. Conventional X-ray films coupled with filters [4], multi-wire proportional counters [5] and X-ray phosphor coupled with photodiodes [6] have all been used experimentally in dual energy X-ray absorptiometry. Scintillators coupled to photomultipliers [2] are most commonly utilized. However, miniaturization for the purpose of constructing arrays is difficult because of their complicated structures. It takes from 350 to 600 sec to measure the bone area by scanning with a point sensor [1], [2].

Semiconductor detectors have the advantages of simplicity and compact size of the detector system due to the direct conversion of photons to electric charge, bypassing the need for photomultipliers. Therefore, semiconductor detectors hold potential for the creation of array which can generate X-ray images in a shorter time than a point sensor. Silicon (Si) based detectors which do not need cooling, and whose spatial resolution is excellent, have been reported by many authors [7]–[9]. However, Si is a low atomic number material ($Z = 14$), and has a low photon detection efficiency. This fact has motivated the development of high efficiency compound semiconductor detectors that have a high energy resolution at room temperature [10]. Cadmium telluride (CdTe) and mercuric iodide (HgI_2) are compound semiconductors. They have high effective atomic numbers (CdTe 48–52, HgI_2 80–53) leading to high detection efficiencies. Due to their large bandgaps (CdTe 1.56 eV, HgI_2 2.13 eV), the thermal generation of carriers at room temperature is low, resulting in low room temperature leakage currents and good room temperature energy resolutions. HgI_2 detectors have been assembled in arrays for a range of applications [11], [12]. Also, a number of CdTe detector arrays have been reported [13]–[16]. They were applied in gamma cameras, position tomography and so on.

We have extended the application of CdTe detectors to X-ray array detectors which are able to obtain both X-ray images in proportion to the intensity of incident X-rays and X-ray energy spectrum information. Using our X-ray imaging sensor with a K-edge filter, we are able to measure both the lower and higher energy photons falling to either side of the K-edge energy of the K-edge filter simultaneously. The two energy X-ray images in the area of 128 mm × 150 mm can be obtained in less than 75 sec by single scanning of the CdTe detector array.

In this paper, we describe a multi-channel CdTe X-ray imaging sensor that has good energy resolution. The construction of both the CdTe detector elements and the X-ray imaging system and their basic characteristics are described. In addition, the use of the X-ray imaging sensor in selective radiographic imaging is reported, and the high speed densitometry of bone phantoms overlying tissue phantoms is demonstrated using the energy subtraction method.

Manuscript received January 24, 1994; revised April 19, 1994.

The authors are with Matsushita Electric Industrial Co., Ltd., Device Process Technology Research Laboratory 3-1-1 Yagumo-nakamachi Moriguchi Osaka, Japan 570.

IEEE Log Number 9402568.

II. Theory of Dual Energy X-Ray Absorptiometry

By using an energy subtraction method, specific elements can be distinguished from their matrix. Moreover, the density can be evaluated if the atomic number differs significantly from that of its matrix. Provided an object consists of substance A and substance B, counts of photons penetrating the object at two photon energies are represented by the following equations:

$$I(E_1) = I_{01} \exp(-\mu_{A1}\rho_A T_A - \mu_{B1}\rho_B T_B) \quad (1)$$

$$I(E_2) = I_{02} \exp(-\mu_{A2}\rho_A T_A - \mu_{B2}\rho_B T_B) \quad (2)$$

where $I(E_1)$, $I(E_2)$, I_{01} and I_{02} are the attenuated and unattenuated X-ray photon numbers, μ_A and μ_B are the mass attenuation coefficients (cm^2/g), ρ_A, ρ_B are the densities (g/cm^3) and T_A and T_B are the thickness' for substance "A" and "B". "1" and "2" indicate the respective energies E_1 and E_2 of the X-ray photons. In (1) and (2), the attenuation coefficients are known, and unattenuated and attenuated X-ray photon numbers can be measured directly. Hence the two densities per unit area $\rho_A T_A$ and $\rho_B T_B$ are unknown quantities. Taking the logarithms of both sides in the above equations, we obtain simplified equations:

$$S(1) = \mu_{A1}\rho_A T_A + \mu_{B1}\rho_B T_B \quad (3)$$

$$S(2) = \mu_{A2}\rho_A T_A + \mu_{B2}\rho_B T_B \quad (4)$$

where

$$S(1) = -\ln(I(E_1)/I_{01}),$$

$$S(2) = -\ln(I(E_2)/I_{02}).$$

Solving (3), (4), we obtain

$$\rho_A T_A = (\mu_{B2}S(1) - \mu_{B1}S(2))/(\mu_{A1}\mu_{B2} - \mu_{B1}\mu_{A2}) \quad (5)$$

$$\rho_B T_B = (\mu_{A1}S(2) - \mu_{A2}S(1))/(\mu_{A1}\mu_{B2} - \mu_{B1}\mu_{A2}) \quad (6)$$

In our measurements, a two component system consisting of bone and tissue is assumed. We can obtain the density per unit area of two substances to measure the attenuated photon numbers at two energy levels using the CdTe X-ray imaging sensor.

III. X-Ray Imaging Sensor

A. CdTe detector element of X-ray imaging sensors

Fig. 1 shows a block diagram of the CdTe detector elements of the X-ray imaging sensors. Each CdTe detector element comprises a CdTe crystal, an amplifier and two sets of discriminators and counters. The resistivity of the CdTe crystals used as detectors was higher than 10^8 (Ω cm). The CdTe wafer was polished and Pt electrodes were formed on each face. It was then cut to 2 mm × 2 mm × 0.5 mm.

The CdTe detector elements were operated in the photon counting mode. To produce X-ray images, a high photon counting rate was needed for the amplifier. We designed a current-voltage conversion type amplifier which has a upper cutoff frequency of 1 MHz. A bias voltage of 120 V was applied to the CdTe crystal to obtain high drift velocities of carriers generated by X-ray photons. The output pulse width was about 0.5 μs at FWHM.

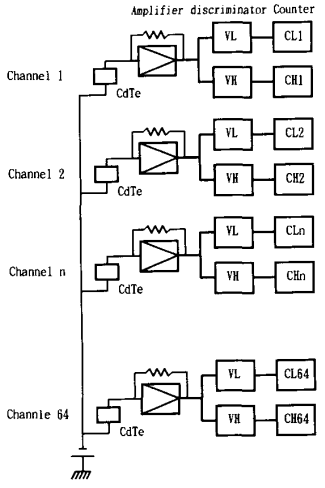

Fig. 1. Block diagram of the CdTe detector elements of the X-ray imaging sensor. VL and VH indicate discrimination voltages which are identical for every channel.

The output pulses were discriminated and separated into two groups according to their heights by means of two sets of discriminators and counters. The total number of pulses of height greater than discrimination voltage VL were counted by Counter CLn. Similarly, pulses higher than VH were counted by Counter CHn.

B. X-ray source and K-edge filter for dual energy X-rays

We used a Shimadzu SHG150G X-ray generator and tube for this evaluation. It was operated in the continuous mode, with a tube voltage of 100 kV. It emitted a fan beam X-ray by means of a slit to prevent the creation of scattered radiation from objects surrounding the X-ray imaging sensor.

The K-edge filter, composed of a 300 μm thick sheet of gadolinium (Gd) and a 100 μm thick sheet of erbium (Er), was placed below the X-ray tube to generate two pseudo-monoenergetic X-ray streams from the broad-band Bremsstrahlung radiation. The simulated spectrum, which was produced by filtering a 100 kV X-ray beam with the K-edge filter, is shown in Fig. 2. The characteristics of the filtered radiation consist of a low energy spike and a high energy hump. The Bremsstrahlung radiation is separated into these two energy levels at about 60 keV since Gd and Er have K-edges of 50.54 keV and 57.20 keV respectively. We irradiated objects with both high and low energy X-ray beams as a dual energy X-ray.

C. X-ray imaging system

Our X-ray imaging sensor has 64 channels, composed of CdTe detector elements arranged in a line with a pitch of

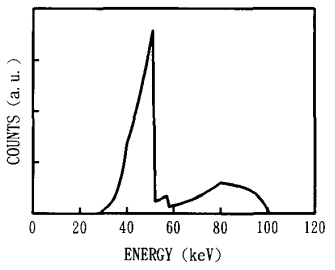

Fig. 2. Simulated spectrum of K-edge filtered X-rays. The K-edge filter was composed of 300 μm gadolinium and 100 μm Erbium and the X-ray tube voltage was 100 kV.

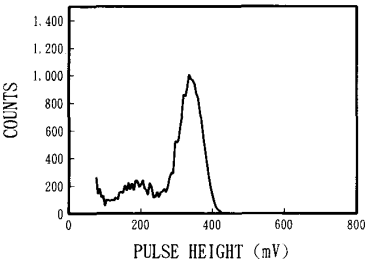

Fig. 3. Pulse height spectrum of ^{241}Am gamma-ray detected by the CdTe detector elements.

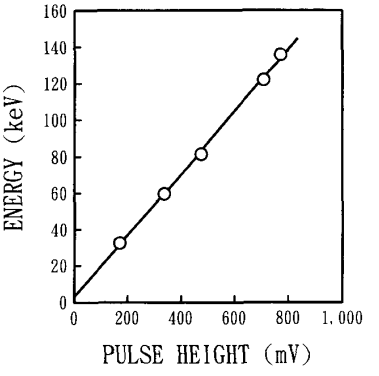

Fig. 4. Photon energy as a function of output pulse height in CdTe detector elements.

2 mm. The count of pulses taken by counters was transferred to a computer. When an object was irradiated with dual energy X-rays produced by the K-edge filter, two transmitted X-ray photon counting images with different energies were taken simultaneously with a single scan, as described below. The numbers of lower and higher energy photons were counted by counters with different discrimination voltages. The discrimination voltage VH was set at the pulse height corresponding to the separation energy in the K-edge filtered X-ray. The discrimination voltage VL was set at above noise level. If the amplitude of pulses from the amplifier was proportional to incident photon energy, the number of the higher energy photons of the dual energy X-ray was counted by Counter CHn. That of the lower one was obtained by subtraction of that of the higher number from the number of photons greater than VL, as counted by Counter CLn.

IV. Experimental Results

A. Energy resolution

The energy resolution of the CdTe detector elements was evaluated from the pulse height spectra of gamma-rays. A ^{241}Am (59.54 keV) gamma-ray source was used to determine pulse height spectra using a single channel analysis technique. Fig. 3 shows the pulse height spectrum of ^{241}Am measured using the CdTe detector elements. A photo peak of 59.54 keV gamma-rays and the escape peaks of Cd and Te K X-rays were observed and clearly resolved around 350 mV and 180 mV, respectively. The energy resolution of the CdTe detector element was estimated from a full-width at half maximum (FWHM) of the photo peak in Fig. 3. The FWHM of the photo peak was 18.7% (11.1 keV). It was similar to the results obtained using a charge sensitive amplifier [17]. The escape peaks were distributed between 27 keV and 37 keV, since the energies of Cd and Te K-X-rays are 22.98 – 26.64 keV and 27.20 – 31.69 keV, respectively. The escape peak count comprised about 23% of total counts.

Fig. 4 shows the pulse heights of the characteristic X- and gamma-ray photo peaks as functions of photon energies from ^{57}Co (122.06 keV, 136.47 keV), ^{133}Ba (81.0 keV, Cs K X-ray 30.62 – 35.82 keV) and ^{241}Am sources. The pulse heights of the photo peaks were proportional to the energies of incident photons in the range of the diagnostic X-ray.

B. Measurement of dual energy X-ray

The pulse height spectrum of dual energy X-rays generated by a CdTe detector element of the X-ray imaging sensor using the single channel analysis technique is shown in Fig. 5. The pulse heights were converted into photon energies according to the relation between incident photon energies and pulse heights shown in Fig. 4. The simulated spectrum of pulse height output from the CdTe detector element is also shown as a dotted line in Fig. 5. The simulation was performed on the following assumptions: 1) The energy resolution of the CdTe detector element was 18.7% at every photon energy. 2) 23% of incident photons cause K X-ray escape. 3) Event appears at the energy 30 keV below that of the incident photon when a K X-ray escapes from the detector element. The agreement between the simulated and the measured spectra was fairly good. In the high energy region, the counts measured using the CdTe detector element were larger than the simulated ones, due to pulse-pileups caused by the high counting rate described below. However, it was clear that the CdTe detector elements were able to obtain the energy information of dual energy X-rays generated by the K-edge filter, maintaining their energy resolution and escape probability at every diagnostic X-ray energy range.

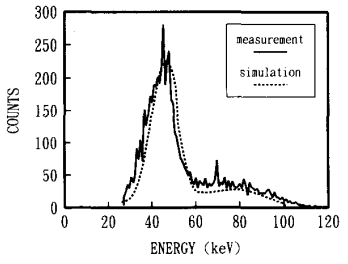

Fig. 5. Measured (solid line) and simulated (dotted line) spectra of dual energy X-ray produced by the K-edge filter in the CdTe detector elements.

To measure simultaneously both low and high energy photons, we set the discrimination voltage VL to 150 mV and VH to 330 mV, corresponding to 28 keV and 60 keV. The counts of photons having energies both higher and lower than the separation energy, $I(H)$ ($I(E_2)$), $I(L)$ ($I(E_1)$) was simply obtained as followed, taking K X-ray escapes into consideration.

$$I(H) = C(H)/(1 - p) \tag{7}$$

$$I(L) = C(L) - \{C(H)/(1 - p)\} \tag{8}$$

where p was a escape probability. We assumed that p was 0.23 at the whole energy.

Fig. 6 shows the counts of both low and high energy photons after penetrating aluminum (Al) on a 15 cm thick acrylic plate as a function of Al thickness. The slopes of $I(L)$ and $I(H)$ were different. We estimated the effective energies of low and high energy X-ray beams by a half-layer method under conditions of 100 kV tube voltage. They were 45 keV and 75 keV, respectively.

Fig. 7 shows linearity to the counting rate of the X-ray imaging sensor. The counting rate was evaluated using whole counts of pulses higher than VL divided by the sampling time. $I(L)$, $I(H)$ was linearly proportional to the number of incident photons below 50 kcps. However, $I(H)$ rapidly increased when the number of incident photons became greater than 50 kcps. This was due to pulse pileup caused by the high pulse rate. $I(L)$ saturated at 50 kcps because it was calculated by subtracting $I(H)$ from the whole counts of pulses. These results indicate that the X-ray imaging sensor maintains its energy resolution at counting rates of up to 50 kcps.

Fig. 8 shows the temperature characteristics of the low and high counts normalized at 25°C. The low and high counts changed by less than 2.5% in the temperature range of 0°C to 40°C. The performance of the CdTe imaging sensor was reliable over a normal temperature range.

C. Application to the dual energy absorptiometry

Using the dual energy absorptiometry with the X-ray imaging sensor, we attempted to take selective images and measure the density of the bone phantoms overlying tissue phantoms. Fig. 9(a) and (b) show a low energy X-ray

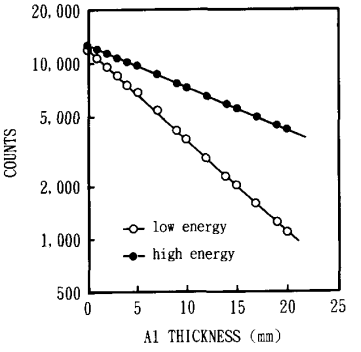

Fig. 6. Attenuation curve of aluminum on a 15 cm acrylic plate for low and high energy X-rays measured using the CdTe detector elements.

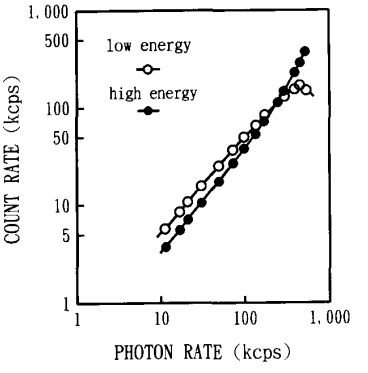

Fig. 7. Linearity of high and low energy X-ray counts to the number of incident photons per second.

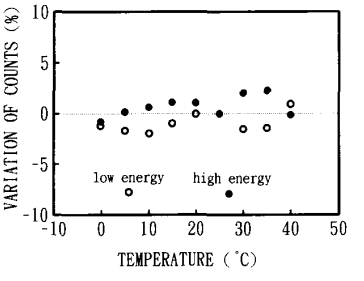

Fig. 8. Temperature characteristics of low and high energy counts in the X-ray imaging sensor.

image and a high energy X-ray image of a hand phantom displayed on a CRT. They were obtained by the scanning X-ray imaging sensor, using a fan beam X-ray under the conditions of X-ray tube voltage 100 kV and current 3 mA. The sampling time of each line was 1.0 sec and the total measuring time was 75 sec. The measuring time was shorter than existing dual energy X-ray systems [1], [2]. Low and high energy images of 64 × 75 pixels were simultaneously produced during the scanning of the X-ray imaging sensor. The contrast in the low energy X-ray image was higher than that in the high energy X-ray

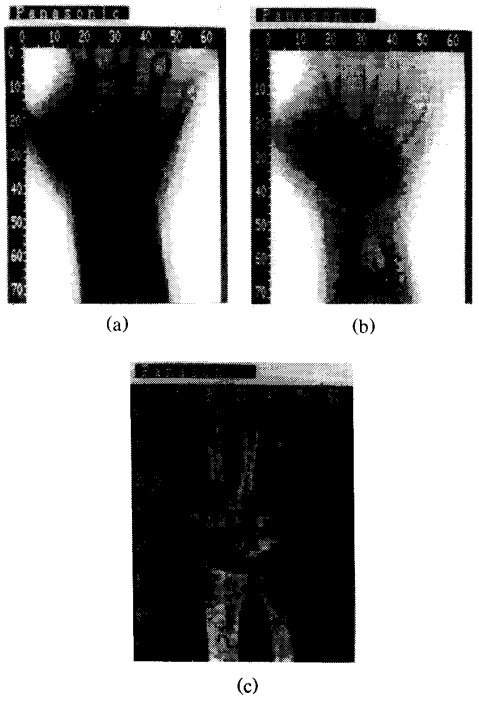

Fig. 9. Selective radiographic images. (a) shows a low energy X-ray image of a hand phantom on an acrylic plate. (b) shows a high energy X-ray image of it. (c) shows a bone mineral density image produced by both low and high energy X-ray images.

image. Calculation based on the theory described above was carried out to obtain the distribution of bone mineral density in the phantom. Fig. 9(c) shows the bone mineral density image on a CRT. Brighter parts of the image indicate higher density. The tissue was completely deleted from the image.

We tested the accuracy and reproducibility using bone equivalent plastic blocks in acrylic plates. Fig. 10 shows the relationship between measured densities and actual densities. The measured densities match the actual densities. The correlation is represented by following equation and the correlation factor is 0.9996:

$$(\text{measured value}) = 0.9302 \cdot (\text{actual value}) + 0.0632. \tag{9}$$

Fig. 11 shows the reproducibility of bone densities measured using the CdTe X-ray imaging sensor. The sampling time of each line in Fig. 11(a) was 1.0 sec and that in Fig. 11(b) was 0.2 sec. The scan time for a measurement of the bone density in the phantom were 75 sec and 15 sec, respectively. The low and high energy counts in the bone region were about 1,300 and 2,100 at the sampling time of 0.2 sec, respectively. The coefficient of variation (CV) was 0.578% in Fig. 11(a) and that in Fig. 11(b) was 0.771%. These results were the same as those in ordinary bone densitometers [1], [2]. The CdTe X-ray imaging sensor obtained good reproducibility in spite of its short scan time.

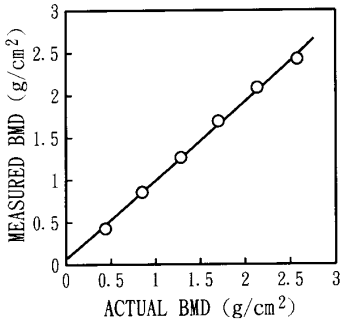

Fig. 10. Demonstration of accuracy of measurement for bone mineral density using the X-ray imaging sensor.

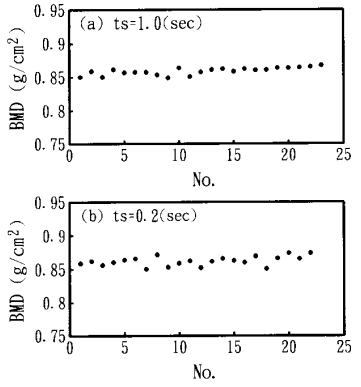

Fig. 11. Reproducibility of bone mineral density measured using the X-ray imaging sensor. (a) sampling time 1.0 sec, (b) sampling time 0.2 sec.

V. Discussion and Conclusions

To realize high speed bone densitometry, arrays or two-dimensional detectors are required that can measure the energies of X-ray photons at different levels. We have developed a 64-channel CdTe X-ray imaging sensor that is able to count the number of dual energy X-rays simultaneously and that has the spatial resolution necessary to carry out quantitative radiography. CdTe detector elements with simple electronic circuits have fairly good energy resolution and adequate counting rate, typical advantages of semiconductor detectors. X-ray imaging sensors can measure not only the intensity but also the energy of the dual energy X-rays. However, the small detector elements of the X-ray array induced a large probability of K X-ray escape. The K X-ray escape peak counts degrade the measured spectrum of dual energy X-rays, and affect the accuracy of bone mineral density measurement. By selecting the separation energy that depends on the materials of the K-edge filter in combination with the maximum photon energy emitted from the X-ray tube, most of the escape counts induced by the higher energy photons of the dual energy X-ray were counted as lower energy counts. As a result of this strategy, the effect of K X-ray escapes was removed using a

simple correction. The X-ray imaging sensor could thus measure bone densities with high accuracy.

One problem in the use of CdTe had been the phenomenon of polarization, which led to instability in the detector performance. However, the CdTe X-ray imaging sensor was very stable in the temperature range of 0°C to 40°C. And CV of the bone mineral densities measured using the X-ray imaging sensor was less than 1% even for about 1,300 counts in the bone region. In spite of the short measuring time, 15 sec, the X-ray imaging sensor has good reproducibility.

The X-ray imaging sensor using CdTe detectors, operated in the photon counting mode, was able to obtain two energy X-ray images simultaneously during a very short measuring time. These features qualify the CdTe imaging sensor, when used with a K-edge filter, for dual energy X-ray absorptiometry. A density image of bone mineral in a two component system was obtained by applying the energy subtraction method and a simple correction for K X-ray escapes. The reproducibility of bone mineral density was reasonably good. The X-ray imaging sensor has presented the potential to be used in high speed bone mineral densitometry.

VI. Acknowledgment

The authors wish to express their sincere appreciation to Mr. Sakae Noda and Mr. Yoshitaka Sunagawa for technical help.

References

[1] I. D. Cullum, P. J. Ell, and J. P. Ryder, "X-ray dual-photon absorptiometry: a new method for the measurement of bone density," *Brit. J. Radiol.*, vol. 62, pp. 587–592, July, 1989.

[2] R. Mazess, B. Collick, J. Tempe, H. Barden, and J. Hanson, "Performance evaluation of a dual-energy X-ray bone densitometer," *Calcif. Tissue. Int.*, vol. 44, pp. 228–232, 1989.

[3] J. L. H. Chan and A. Macovski, "Application of filtered bremsstrahlung spectra in radiologic studies, part 1: Spectrum properties and optical energies," *IEEE Trans. Nucl. Sci.*, vol. NS-24, pp. 1968–1976, Aug. 1977.

[4] G. T. Barnes, R. A. Sones, M. M. Tesic, D. R. Morgan, and J. N. Sanders, "Detector for dual-energy digital radiography," *Radiol.*, vol. 156, pp. 537–540, Aug. 1989.

[5] F. Angelini, R. Bellazzini, A. Brez, M. M. Massi, M. R. Torquati, G. Perri, D. Trippi, and F. Beghe, "Bone densitometry of the peripheral skeleton with a new photon counting and imaging device," *Invest. Radiol.*, vol. 24, pp. 684–691, Sept. 1989.

[6] K. Engelke, M. Lohmann, W. R. Dix, and W. Graeff, "A system for dual energy microtomography of bones," *Nucl. Instr. and Meth.* A274, pp. 380–389, 1989.

[7] S. A. Audet, E. M. Schooneveld, S. E. Wouters, and M. H. Kim, "High-purity silicon soft X-ray imaging sensor arrays," *Sensors and Actuators*, vol. A21–A23, pp. 482–486, 1990.

[8] I. Fujieda, S. Nelson, R. A. Street, and R. L. Weisfield, "Radiation imaging with 2D a-Si sensor arrays," *IEEE Trans. Nucl. Sci.*, vol. NS-39, pp. 1056–1062, 1992.

[9] Y. Naruse, T. Sugita, T. Kobayashi, M. Jimbo, M. Fujii, Y. Yoshida, and T. Suzuki, "Multichannel semiconductor detectors for X-ray transmission computed tomography," *IEEE Trans. Nucl. Sci.*, vol. NS-27, pp. 252–256, Feb. 1980.

[10] M. Cuzin, "Some new developments in the field of high atomic number materials," *Nucl. Instr. Meth.*, vol. A253, pp. 407–417, 1987.

[11] D. A. Ordendahl, L. Kaufman, K. Hoseir, L. Padgett, and C. Ortale, "Operating characteristics of small position-sensitive mercuric iodide detectors," *IEEE Trans. Nucl. Sci.*, vol. NS-29, pp. 784–788, 1982.

[12] J. S. Iwanczyk, W. K. Warburton, A. J. Dabrowski, B. Hedman, K. O. Hodgson, and B. E. Patt, "Development of mercuric iodide energy dispersive X-ray array detectors," *IEEE Trans. Nucl. Sci.*, vol. NS-35, pp. 93–97, 1988.

[13] G. Entine, R. Luthmann, W. Mauderli, L. T. Fitzgerald, and C. M. Williams, "Cadmium telluride gamma camera," *IEEE Trans. Nucl. Sci.*, vol. NS-26, pp. 552–558, 1979.

[14] D. Chu, L. Kaufman, K. Hoiser, and J. Hoenninger, "An evaluation of cadmium tellurude detectors for computer assisted tomography," *J. Comp. Assisted Tomog.*, vol. 2, pp. 586–593, Nov. 1978.

[15] F. Casali, D. Bollini, P. Chirco, M. Rossi, G. Baldazzi, W. Dusi, E. Caroli, G. Dicocco, A. Donati, G. Landini, and J. B. Stephen, "Characterization of small CdTe detectors to be used for linear and matrix arrays," *IEEE Trans. Nucl. Sci.*, vol. NS-39, pp. 598–604, 1992.

[16] G. Entine, P. Waer, T. Tiernan, and M. R. Squillante, "Survey of CdTe nuclear detector application," *Nucl. Instr. Meth.*, vol. A283, pp. 282–290, 1989.

[17] T. Shoji, T. Taguchi, K. Ohba, and Y. Hiratate, "Characteristics of MSM-Type CdTe γ-ray detector fabricated from undoped p-Type crystals," *Phys. Stat. Sol.* (a), vol. 57, pp. 765–774, 1980.